

# Neutral current quasielastic (anti)neutrino scattering beyond the Fermi gas model at MiniBooNE and BNL kinematics

M.V. Ivanov<sup>1</sup> A.N. Antonov<sup>1</sup> M.B. Barbaro<sup>2,3</sup> C. Giusti<sup>4</sup>  
A. Meucci<sup>4</sup> J.A. Caballero<sup>5</sup> R. González-Jiménez<sup>6</sup>  
E. Moya de Guerra<sup>6</sup> J.M. Udías<sup>6</sup>

<sup>1</sup>Institute for Nuclear Research and Nuclear Energy, Bulgarian Academy of  
Sciences, Sofia, Bulgaria

<sup>2</sup>Università di Torino and INFN, Torino, Italy

<sup>3</sup>Université Paris-Saclay, CNRS/IN2P3, IJCLab, Orsay cedex, France

<sup>4</sup>Università degli Studi di Pavia and INFN, Pavia, Italy

<sup>5</sup>Universidad de Sevilla, Sevilla, Spain

<sup>6</sup>Universidad Complutense de Madrid, Madrid, Spain

- I. Introduction
- II Theoretical scheme
- III. Results and discussion
- IV. Conclusions

- I. Introduction
- II Theoretical scheme
- III. Results and discussion
- IV. Conclusions



M.V. Ivanov, A.N. Antonov, J.A. Caballero *et al.*, Phys. Rev. C **89**, 014607 (2014).



M.V. Ivanov, A.N. Antonov, M.B. Barbaro *et al.*, Phys. Rev. C **91**, 034607 (2015).

In most neutrino experiments, the interactions of the neutrinos occur with nucleons bound in nuclei. Model predictions for these reactions involve many different effects (nuclear correlations, interactions in the final state, possible modification of the nucleon and nucleon resonances properties inside the nuclear medium) that presently cannot be computed in a unambiguous and precise way.

One way of avoiding model-dependencies is to use the nuclear response to other leptonic probes, such as electrons, under similar conditions than the neutrino experiments. This is justified on the success of the scaling ideas and the observation of superscaling in electron-nucleus scattering.

The SuSA method relies on the superscaling properties of the electron scattering data: at sufficiently high momentum transfer the inclusive differential ( $e, e'$ ) cross sections, divided by a suitable function which takes into account the single nucleon content of the problem:

$$f = \frac{d^2\sigma/d\Omega dk'}{S(q, \omega)}, \quad (1)$$

depend only upon one kinematical variable:

$$\psi_{\text{QE}} = \pm \sqrt{\frac{1}{2T_F} \left( q \sqrt{1 + \frac{1}{\tau}} - \omega - 1 \right)}, \quad (2)$$

the scaling variable (this behavior is called scaling of first kind) and the resulting function is roughly the same for all nuclei (scaling of second kind). When both kinds of scaling are fulfilled the cross section is said to superscale.

Imposed necessity to include the effects of nuclear dynamics, NN correlations, final state interactions (FSI), approaches beyond the impulse approximation (IA), contributions of 2p-2h and 3p-3h processes, to test the value of axial mass ( $M_A = 1.032 \text{ GeV}^2$ , or 1.28, or 1.35 ...), to apply the phenomenological SuSA approach, the relativistic mean field (RMF) method, the relativistic Green's function (RGF) method, the coherent density fluctuation model (CDFM), realistic spectral functions, to test the role of the strangeness content of the nucleon and others.

## Our interest:

- To analyze NCQE neutrino cross sections on  $^{12}\text{C}$  measured by MiniBooNE (Aguilar-Arevalo *et al.*, 2010) and by BNL E734 experiment (Abe *et al.*, 1983, 1986, and Ahrens *et al.*, 1987), as well as antineutrino-nucleus scattering by MiniBooNE (Aguilar-Arevalo *et al.*, 2013, 2015).

## II. Theoretical scheme



Within PWIA (Caballero *et al.*, 2010; A.N. Antonov *et al.*, 2011) the  $(e, e'N)$  differential cross section factorizes in two basic terms: the electron-nucleon cross section for a moving, off-shell nucleon and the spectral function that gives the combined probability to find a nucleon of certain momentum and energy in the nucleus:

$$\left[ \frac{d\sigma}{d\epsilon' d\Omega' dp_N d\Omega_N} \right]_{(e, e'N)}^{PWIA} = K \sigma^{eN}(q, \omega; p, \mathcal{E}, \phi_N) S(p, \mathcal{E}) \quad (3)$$

with  $K$  a kinematical factor and where  $p$  is the missing momentum and  $\mathcal{E}$  the excitation energy, essentially the missing energy minus the separation energy.

Two assumptions: the spectral function is assumed to be isospin independent, and second  $\sigma^{eN}$  is assumed to have a very mild dependence on the missing momentum and excitation energy. The differential cross section for inclusive QE ( $e, e'$ ) processes is written in the form:

$$\left[ \frac{d\sigma}{d\epsilon' d\Omega'} \right]_{(e, e')} \cong \bar{\sigma}^{eN}(q, \omega; p = |y|, \mathcal{E} = 0) F(q, \omega), \quad (4)$$

$$\bar{\sigma}^{eN} \equiv K \sum_{i=1}^A \int d\phi_{N_i} \frac{\sigma^{eN_i}}{2\pi}. \quad (5)$$

In PWIA

$$F(q, \omega) = 2\pi \iint_{\Sigma(q, \omega)} p dp d\mathcal{E} S(p, \mathcal{E}), \quad (6)$$

$\Sigma(q, \omega)$  is the kinematically allowed region.

In RFG:

$$y_{RFG} = m_N \left( \lambda \sqrt{1 + \frac{1}{\tau}} - \kappa \right), \quad (7)$$

where

$$\kappa \equiv q/2m_N, \quad \lambda \equiv \omega/2m_N, \quad \tau \equiv |Q^2|/4m_N^2 = \kappa^2 - \lambda^2.$$

$$\psi = \frac{1}{\sqrt{\xi_F}} \frac{\lambda - \tau}{\sqrt{(1 + \lambda)\tau + \kappa\sqrt{\tau(1 + \tau)}}}, \quad (8)$$

where

$$\xi_F = \sqrt{1 + \eta_F^2} - 1 \quad \text{and} \quad \eta_F = k_F/m$$

$$f_{RFG}(\psi) = \frac{3}{4}(1 - \psi^2)\Theta(1 - \psi^2) \quad (9)$$

**Indeed the analyses of the world data on inclusive electron-nucleus scattering confirmed the observation of this phenomenon and thus allowed to extract a universal nuclear response to weak interacting probes.**

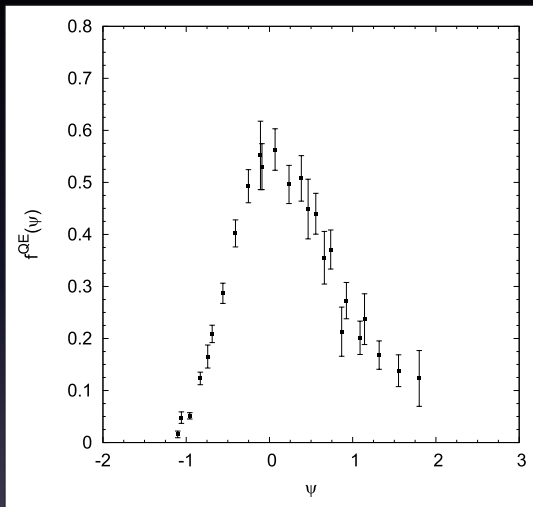


Figure:  $f(\psi)$  for  $^{12}\text{C}$ , the longitudinal experimental data.

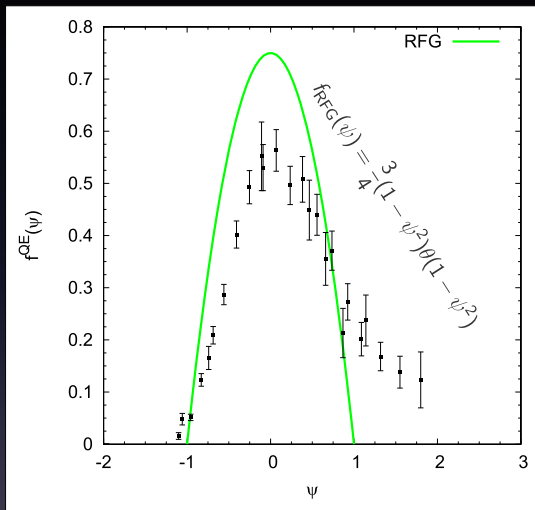


Figure:  $f(\psi)$  for  $^{12}\text{C}$ , RFG, as well as the longitudinal experimental data.

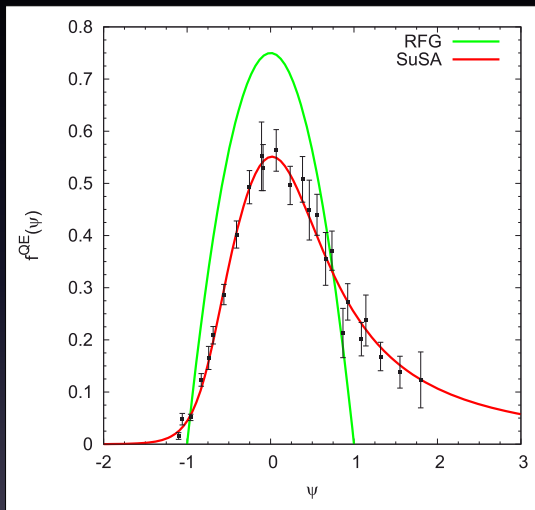


Figure:  $f(\psi)$  for  $^{12}\text{C}$ , RFG, SuSA, as well as the longitudinal experimental data.

The spectral function (A.N. Antonov, M.V. Ivanov *et al.*, 2011):

i) Independent particle shell model (IPSM):

$$S_{IPSM}(p, \mathcal{E}) = \sum_i 2(2j_i + 1)n_i(p)\delta(\mathcal{E} - \mathcal{E}_i) \quad (10)$$

ii) Beyond mean-field approximation

$$S(p, \mathcal{E}) = \sum_i 2(2j_i + 1)n_i(p)L_{\Gamma_i}(\mathcal{E} - \mathcal{E}_i) \quad (11)$$

$$L_{\Gamma_i}(\mathcal{E} - \mathcal{E}_i) = \frac{1}{\pi} \frac{\Gamma_i/2}{(\mathcal{E} - \mathcal{E}_i)^2 + (\Gamma_i/2)^2} \quad (12)$$

iii)  $n_i(p)$  : s.p. momentum distributions of HO shell – model  
s.p. state  $i$ ;



- iv)  $n_i(p)$  : including short-range NN correlations using natural orbitals (NO),  $\varphi_\alpha(r)$  being s.p. wave functions, defined by Löwdin (1955) as a complete orthonormal set of s.p. wave functions that diagonalize the one-body density matrix:

$$\rho(\mathbf{r}, \mathbf{r}') = \sum_a N_\alpha \varphi_\alpha^*(\mathbf{r}) \varphi_\alpha(\mathbf{r}'), \quad (13)$$

$$0 \leq N_\alpha \leq 1, \quad \sum_\alpha N_\alpha = A$$

We use  $\varphi_\alpha(r)$  within the lowest-order approximation of the Jastrow correlation method (M.V. Stoitsov, A.N. Antonov, S.S. Dimitrova, 1993).

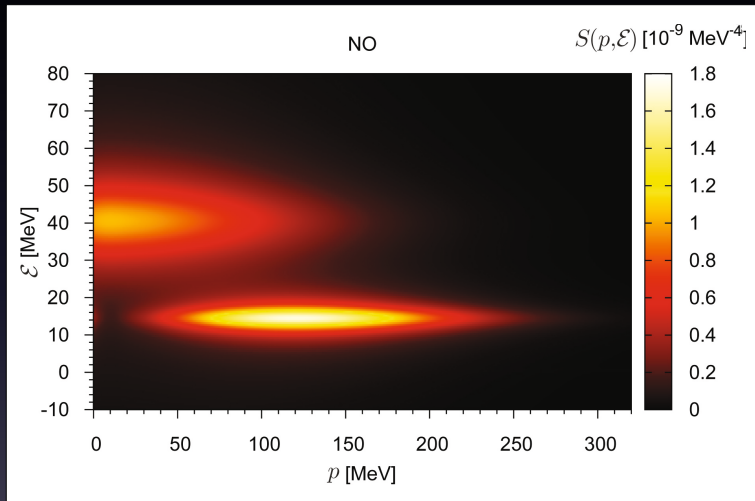


Figure: The  $^{12}\text{C}$  realistic  $S(p, \mathcal{E})$  using natural orbitals single-particle  $n_i(p)$  from the Jastrow correlation method and Lorentzian function for the energy dependence. Two shells  $1p$  and  $1s$  are clearly visible.

Final-state interaction (FSI)

We follow the approximation of Ankowski, Sobczyk (2008) for inclusive electron scattering with two types FSI: the Pauli blocking and the interaction of the struck nucleon with the spectator system with time-independent optical potential (OP):

$$U = V - iW \quad (14)$$

FSI is accounted for by replacing the  $\delta$ -function in the PWIA expression for the inclusive electron - nucleus cross section

$$\frac{d\sigma_t}{d\omega d|\mathbf{q}|} = 2\pi\alpha^2 \frac{|\mathbf{q}|}{E_k^2} \int dE d^3p \frac{S_t(\mathbf{p}, E)}{E_p E_{p'}} \times \\ \times \delta(\omega + M - E - E_{p'}) L_{\mu\nu}^{\text{em}} H_{\text{em}, t}^{\mu\nu} \quad (15)$$

by (Horikawa *et al.*, 1980)

$$\delta(\omega + M - E - E_{p'}) \rightarrow \frac{W/\pi}{W^2 + [\omega + M - E - E_{p'} - V]^2} \quad (16)$$

$t$  – isospin,  $L_{\mu\nu}^{\text{em}}$  – leptonic tensor,  $H_{\text{em},t}^{\mu\nu}$  – hadronic tensor  
 $V$  and  $W$  are obtained (Cooper *et al.*, 1993) from Dirac OP.  
 $U(p')$  related to the scalar ( $S$ ) and vector ( $V$ ) parts of OP is  
 obtained in the form

$$E_{\mathbf{p}'} + U(\mathbf{p}') = \sqrt{[M + S(T_{\mathbf{p}'}, \bar{r}_S)]^2 + \mathbf{p}'^2} + V(T_{\mathbf{p}'}, \bar{r}_V) \quad (17)$$

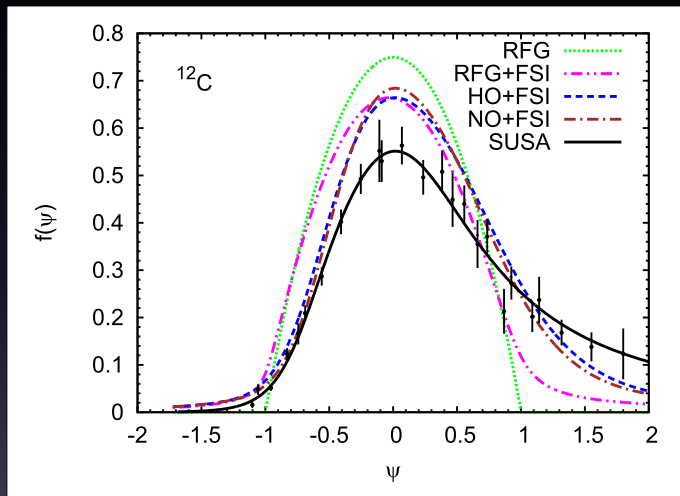
Alternatively, OP with  $W$  (Nakamura *et al.*, 2005)

$$W = \frac{\hbar c}{2} \rho_{\text{nucl}} \sigma_{NN} \frac{|\mathbf{p}'|}{E_{\mathbf{p}'}} \quad (18)$$

In the present work we use Eq. (17).

The procedure:

- (i) The spectral function  $S(p, \mathcal{E})$  (Eq. (11)) with  $L_{\Gamma_i}$ ;
- (ii)  $n_i(p)$  corresponding to the HO single-particle wave functions or to the NOs from the Jastrow correlation method;
- (iii) The Lorentzian function [Eq. (12)] is used with parameters  $\Gamma_{1p} = 6$  MeV,  $\Gamma_{1s} = 20$  MeV, fixed to the experimental widths of the  $1p$  and  $1s$  states in  $^{12}\text{C}$  (Dutta, 1999);
- (iv) For a given  $q = 1$  GeV/c and  $\varepsilon = 1$  GeV electron-nucleus ( $^{12}\text{C}$ ) cross section (Eq. (15)) with  $S(p, \mathcal{E})$  (Eq. (11));
- (v)  $F(q, \omega)$  from Eq. (4) is calculated and multiplying it by  $k_A$  the scaling function  $f(\psi)$  is obtained;
- (vi) For accounting FSI, the  $\delta$ -function in Eq. (15) is replaced by Eq. (16) and Eq. (17).

Figure:  $f(\psi')$  for  $^{12}\text{C}$ , RFG+FSI, HO+FSI, NO+FSI, SuSA

# III. Results and discussion

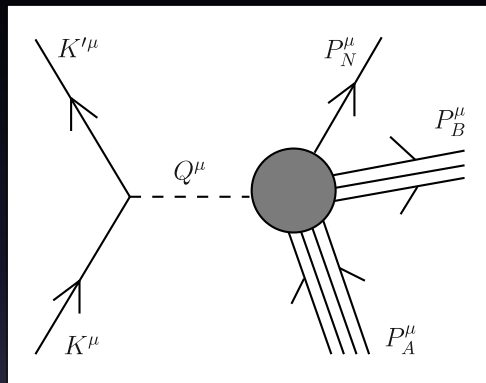


Figure: Kinematics for semi-leptonic nucleon knockout reactions in the one-boson approximation. Lepton  $K^\mu = (\epsilon, \mathbf{k})$  scatters to another lepton  $K'^\mu = (\epsilon', \mathbf{k}')$ ; In the laboratory system the initial nucleus  $P_A^\mu = (M_A^0, 0)$ , final hadronic state is a proton or neutron with  $P_{N=p \text{ or } n}^\mu = (E_N, \mathbf{p}_N)$  and an unobserved residual nucleus  $P_B^\mu = (E_B, \mathbf{p}_B)$ .



- QE electron or CCQE neutrino scattering (the outgoing lepton is observed and sum over nucleon variables is performed):  
 “t-channel” reactions, since the Mandelstam variable  $t = (K^\mu - K'^\mu)^2$  is fixed.
- NC neutrino scattering (only the outgoing  $N$  is observed and the outgoing  $\nu$  is integrated over):  
 “u-channel” process, where the Mandelstam variable  $u = (K^\mu - P_N^\mu)^2$  is fixed.  
 The kinematics is not the same as in  $(e, e')$ .  
 $Q^\mu = (\omega, \vec{q})$  is not specified.  
 New transfer 4-momentum  $Q'^\mu = K^\mu - P_N^\mu = (\omega', \vec{q}')$  is introduced and new scaling variables  $y^{(u)}(q', \omega')$  and  $\psi^{(u)}(q', \omega')$  are defined.

Found: the 2<sup>nd</sup> type scaling is excellent, 1<sup>st</sup> type is good in some kinematics ( $> 50$  deg).

So, 1<sup>st</sup> type scaling is expected (when the cross section is integrated over the angles and it reaches large values) to work properly at MiniBooNE and BNL (based on  $u$ -channel).

### In PWIA

$(l, l'N)$  (Amaro *et al.*, 2006):

$$\frac{d\sigma}{d\Omega_N dp_N} \simeq \bar{\sigma}_{s.n.}^{(u)} F(y', q') \quad (1)$$

$$F(y', q') \equiv \int_{\mathcal{D}_u} p dp \int \frac{d\mathcal{E}}{E} \Sigma \simeq F(y') \quad (2)$$

$$\overline{\sigma}_{\text{s.n.}}^{(u)} = \frac{1}{32\pi\epsilon} \frac{1}{q'} \left( \frac{p_N^2}{E_N} \right) g^4 \int_0^{2\pi} \frac{d\phi'}{2\pi} l_{\mu\nu}(\mathbf{k}, \mathbf{k}') w^{\mu\nu}(\mathbf{p}, \mathbf{p}_N) D_V(Q^2)^2 \quad (3)$$

- $D_V(Q^2)$  – vector boson propagator;
- $Q'^{\mu} \equiv K^{\mu} - P_N^{\mu} = (\omega', \mathbf{q}')$  – four-momentum transferred from the initial lepton to the ejected nucleon;
- $y'$  – scaling variable ( $u$ -channel);
- **Assumption:** the domains of integration  $D_u$  and  $D_t$  are very similar. Then the scaling function from electron scattering ( $D_t$ ) can be used for NC neutrino scattering;
- $D_t$  and  $D_u$  differ significantly only at large  $\mathcal{E}$ .

Analyses of NCQE on CH<sub>2</sub> target measured by MiniBooNE and BNL E734 (target: 79% protons in <sup>12</sup>C and aluminum and 21% of free protons).

### III. Results and discussion

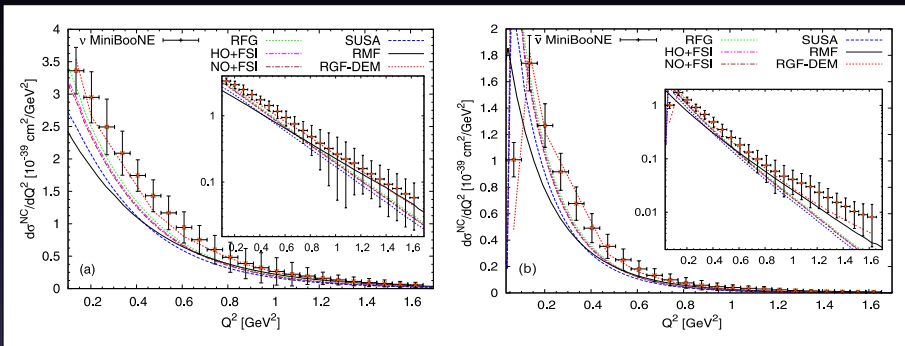


Figure: NCQE (a)  $\nu N \rightarrow \nu N$  and (b)  $\bar{\nu} N \rightarrow \bar{\nu} N$  flux-averaged differential cross section;  $M_A = 1.032 \text{ GeV}$ ;  $\Delta s = 0$ ;  $Q^2 = 2M_N T_N$ .

Underestimations for all models for  $\nu$  except RGF-DEM in  $0.1 < Q^2 < 0.7 \text{ GeV}^2$  and are within error bars for higher  $Q^2$ . The same models underestimate data at high  $Q^2$  for the antineutrino case.

RGF accounts for imaginary part of the optical potential that is not included in other models.

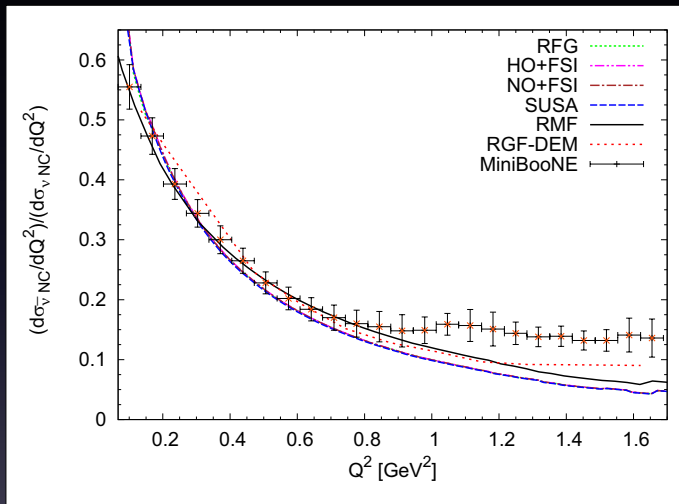


Figure: Ratio of  $\bar{\nu}$  to  $\nu$  NCQE using RFG, HO+FSI, NO+FSI, SuSA, RGF-DEM, RMF, and comparison with MiniBooNE data (MiniBooNE, 2015).

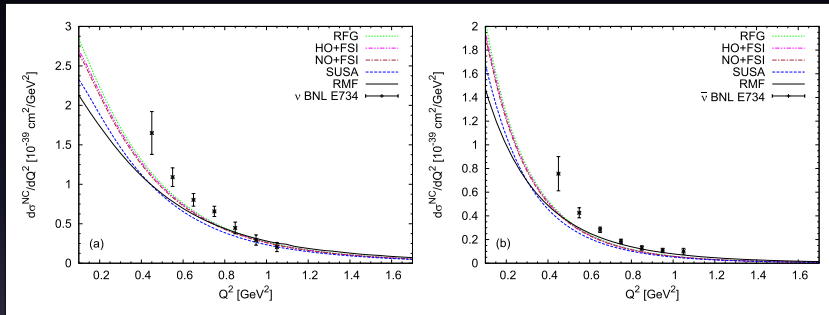


Figure: NCQE flux-averaged cross section: (a)  $\nu p \rightarrow \nu p$  and (b)  $\bar{\nu} p \rightarrow \bar{\nu} p$  compared with the BNL E734 experimental data (Abe *et al.*, 1983, 1986; Ahrens *et al.*, 1987);  $M_A = 1.032 \text{ GeV}^2$ ;  $\Delta s = 0$ .



#### Results:

- 1) NO and HO with and without FSI give similar results (FSI leads to a small change);
- 2) The correlation and non- correlation approaches give results with small differences. Thus, the process is not too sensitive to the specific treatment of the bound state.

### III. Results and discussion

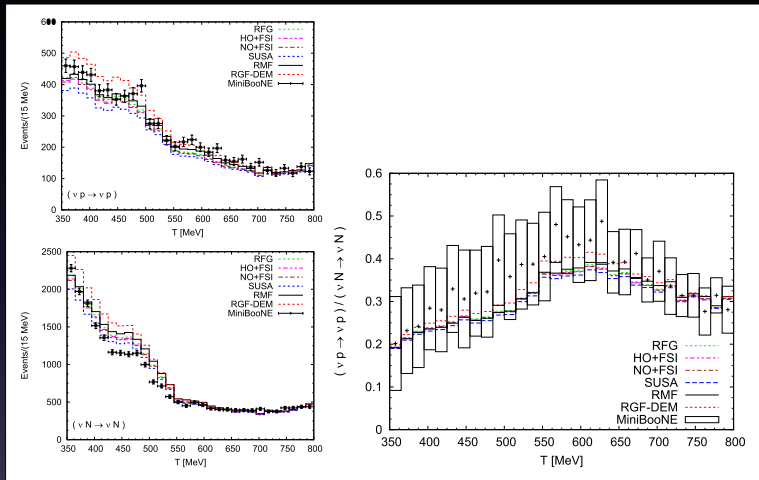


Figure: The RFG, HO+FSI, NO+FSI, SUSA, RGF, and RMF predictions, after the folding procedure, compared with the histograms of the numerator (top-left panel) and denominator (bottom-left panel) of the ratio. The corresponding ratio is shown in the right panel of the figure.

## IV. Conclusions

### For NCQE $\nu(\bar{\nu}) + {}^{12}\text{C}$ analyses

- 1) In NCQE there is no information on  $E$  and  $p$  of the ejected neutrino and thus, the 4-transferred momentum cannot be determined. Some caution should be drawn concerning the “validity” of scaling arguments when applied to NC, though our previous studies give us a confidence.
- 2) We use  $S(p, \mathcal{E})$  with included short-range  $NN$  correlations and realistic  $\mathcal{E}$ -dependence and compare the results also with those from SuSA, RMF, and the RGF approaches, as well as with the data from MiniBooNE and BNL E734.

### For NCQE $\nu(\bar{\nu}) + {}^{12}\text{C}$ analyses

- 3) The inclusion of FSI in  $S(p, \mathcal{E})$ -based calculations leads to a small depletion of cross section in agreement with those of RFG model. The FSI effects in the RGF model lead to larger cross section in agreement with data. On the contrary, the SuSA and RMF approaches lead to smaller differential cross sections at low  $|Q^2| \leq 0.6\text{--}0.8 \text{ GeV}^2$ . Particular sensitivity of NC to the specific description of FSI effects is shown.

### For NCQE $\nu(\bar{\nu}) + {}^{12}\text{C}$ analyses

- 4) Our calculations are based on the impulse approximation. They do not include *e.g.*, 2p-2h contributions induced by MEC that are very important in the neutrino-nuclei scattering processes. They give a significant enhancement in the cross sections at low to moderate values of  $Q^2$ . Particular studies are necessary of the different role played by 2p-2h contributions and MEC in the case of neutrino- or antineutrino-nuclei processes.

THANK YOU VERY MUCH FOR  
YOUR ATTENTION !!!